# Reno-protective ameriolations of *Mirabilis himalaica* in mice with cisplatin induced injury

Jingrui Ji<sup>1,2,4†</sup>, Xiangdong Wang<sup>1,2,4†</sup>, Shuai Lian<sup>1,2,4</sup>, Haoyang Nie<sup>1,2,4</sup>, Fa Shi<sup>1,2,4</sup>, Fei Peng<sup>1,2,4</sup>, Mingxuan Zhao<sup>1,2,4</sup>, Ziauddin³, Hongliang Zhang<sup>1,2,4\*</sup>, Peng Shang<sup>1,2,4\*</sup>

<sup>1</sup>College of Animal Science, Xizang Agriculture and Animal Husbandry University, Linzhi 860000, Xizang, China
 <sup>2</sup>Key Laboratory of Tibetan Pig Genetic Improvement and Reproduction Engineering, Linzhi 860000, Xizang, China
 <sup>3</sup>Center for Advanced Studies in Vaccinology & Biotechnology (CASVAB), University of Balochistan, Quetta, Pakistan
 <sup>4</sup>Center for Provincial Departmental Collaborative Innovation of Xizang Characteristic Agriculture and Animal Husbandry Resources Research and Development, Linzhi 860000, Xizang, China

†These authors contributed equally to this work \*Corresponding author's email: holingzhang@126.com; shangpeng1984@xza.edu.cn Received: 17 June 2025 / Accepted: 23 September 2025 / Published Online: 10 October 2025

#### **Abstract**

Cisplatin is a widely used chemotherapeutic, yet its clinical use is limited by severe nephrotoxicity that often causes acute kidney injury (AKI). Effective, safe strategies to mitigate this remain unmet. We investigated the protective effect of Mirabilis himalaica extract (MHE) against cisplatin-induced acute kidney injury (AKI) in mice and explored its underlying mechanisms. Fifty mice were divided into five groups: control negative, cisplatin model (Control positive with 10 mg/kg), and three MHE treatment groups (10, 15, 20 mg/kg/day) following cisplatin (10 mg/kg). Controls and the model group received saline orally; treatment groups received MHE for 14 days. We measured serum creatinine (Cr), blood urea nitrogen (BUN), and β2-microglobulin (β2-MG) levels. Renal histopathology was assessed using H&E staining. Compared to the cisplatin model group, the medium-dose MHE group (15 mg/kg) significantly reduced serum Cr (41.8%, P < 0.01), BUN (24.5%, P < 0.01), and  $\beta$ 2-MG levels (17.3%, P < 0.01). Histopathological analysis confirmed that medium-dose MHE markedly attenuated cisplatin-induced renal tubular damage, including epithelial cell swelling, necrosis, and inflammatory infiltration. While high-dose MHE (20 mg/kg) showed a trend in reducing β2-MG, this effect was not statistically significant. Low-dose MHE (10 mg/kg) did not demonstrate significant protection. MHE dose-dependently ameliorates cisplatin-induced AKI in mice, with optimal efficacy observed at 15 mg/kg. The renoprotective effects are associated with attenuation of renal dysfunction and histological damage, potentially mediated through suppression of oxidative stress and inflammation. These findings support MHE as a promising candidate for further development as a natural therapeutic agent against AKI.

**Keywords**: Acute Renal injury, Cisplatin, Inflammatory response, *Mirabilis himalaica*, Oxidative stress

#### How to cite this article:

Ji J, Wang X, Lian S, Nie H, Shi F, Peng F, Zhao M, Ziauddin, Zhang H and Shang P. Reno-protective ameriolations of *Mirabilis himalaica* in mice with cisplatin induced injury. Asian J. Agric. Biol. 2025: e2025117. DOI: https://doi.org/10.35495/ajab.2025.117

This is an Open Access article distributed under the terms of the Creative Commons Attribution 4.0 License. (https://creativecommons.org/licenses/by/4.0), which permits unrestricted use, distribution, and reproduction in any medium, provided the original work is properly cited.

#### Introduction

Cisplatin, representative platinum-based chemotherapeutic agent, has played an irreplaceable role in treating lung, ovarian, testicular, and other solid tumors since its clinical introduction in the 1970s. It exerts its cytotoxic effect by forming DNA intrastrand cross-links, thereby blocking DNA replication and transcription (Chao et al., 2020). Cisplatin has significantly prolonged survival times for cancer patients and remains a cornerstone of modern chemotherapy regimens (Sugarbaker et al., 2013; Raudenska et al., 2019; Romani, 2022). However, its clinical utility is severely limited by dose-dependent nephrotoxicity, with approximately 30% of treated patients developing acute kidney injury (AKI) (Manohar and Leung, 2018; Zhu et al., 2023; Elmorsv et al., 2024). Research indicates that cisplatin nephrotoxicity involves multiple pathological mechanisms: The drug accumulates in renal tubular epithelial cells via systemic circulation, directly damaging mitochondrial membrane potential, inducing mitochondrial dysfunction and reactive oxygen species (ROS) burst, leading to oxidative stress. Excessive ROS activates the NF-kB signaling pathway (Yang et al., 2022), triggering a cascade of pro-inflammatory cytokines such as tumor necrosis factor-alpha (TNF-α) and interleukin-6 (IL-6), thereby exacerbating the inflammatory microenvironment. Concurrently, cisplatin disrupts the Bax/Bcl-2 protein equilibrium (Yu et al., 2018; Raghav et al., 2019; Zhao et al., 2024), inducing cytochrome C release and activating the caspase cascade, ultimately promoting Bax/Bcl-2-mediated cellular apoptosis (Liu et al., 2020; Jiang et al., 2022). Current clinical interventions, including hydration therapy (HT) and antioxidants (e.g., N-acetylcysteine, NAC), offer limited renal protection and may compromise cisplatin's antitumor efficacy (Gómez-Sierra et al., 2018; Wang et al., 2021). Furthermore, hydration therapy can increase cardiac load and induce electrolyte disturbances, antioxidant while interventions might interfere with cisplatin's ROSdependent antitumor mechanisms, potentially reducing chemotherapeutic effectiveness. Against this backdrop, Traditional Chinese Medicine (TCM), which leverags its unique multi-component and multitarget synergistic approach (Luan et al., 2020; Li et al., 2021), offers promising strategies for preventing and treating kidney diseases. Specifically, Mirabilis himalaica (Edgew.) Heimerl, recognized as one of the

"five roots" in Tibetan medicine, boasts centuries of clinical use. Traditional texts document its properties for warming the kidneys, promoting yang, inducing diuresis, enhancing lymphatic flow, and alleviating calculi and pain (Shao et al., 2020). Modern pharmacological studies have identified its active constituents, including flavonoids (e.g., Boeravinone B, D), alkaloids, and tianshic acid, which confer antioxidant, anti-inflammatory, and anti-fibrotic effects through synergistic pathways (Li et al., 2023; Chen et al., 2025). For instance, Boeravinone B significantly enhances cellular antioxidant defenses by activating the Nrf2/ARE pathway and upregulating enzymes like superoxide dismutase (SOD) and glutathione peroxidase (GPx), while tianshic acid specifically inhibits caspase-3 activation in renal tubular epithelial cells (Miao et al., 2018), blocking apoptotic signaling and reducing parenchymal damage (Sablania et al., 2019; Wang et al., 2021). Preliminary studies indicate Mirabilis himalaica extract (MHE) exhibits renal protective effects in chronic conditions like diabetic nephropathy and ischemia-reperfusion injury. However, its efficacy against cisplatin-induced AKI—a common clinical complication—remains systematically unevaluated, particularly regarding dose-response relationships, optimal intervention timing, and underlying molecular mechanisms.

Cisplatin-induced acute kidney injury (AKI) constitutes a critical hurdle to effective cancer chemotherapy: it not only elevates patient morbidity and mortality but also compels clinicians to reduce cisplatin dosages or terminate treatment entirely directly undermining the antitumor efficacy of chemotherapy—and given the limitations of current interventions (i.e., inadequate renal protection and potential compromise of cisplatin's therapeutic effects), developing novel agents that confer robust renal protection without impairing cisplatin's anticancer activity remains an urgent, unmet clinical imperative in oncology, one whose address will directly enhance cancer patients' survival rates and quality of life while optimizing cisplatin-based chemotherapy regimens to boost their clinical utility. From an academic standpoint, this study bridges a key gap in existing research by systematically evaluating the efficacy of Mirabilis himalaica extract (MHE) against cisplatin-induced AKI—an area that has yet to be thoroughly explored—while also capitalizing on the underutilized potential of Tibetan medicine (a vital branch of traditional Chinese medicine, TCM) in modern pharmacology: by validating MHE's

nephroprotective effects and elucidating its underlying mechanisms, the research furnishes robust experimental evidence and a theoretical basis for the modern pharmacological investigation of traditional Tibetan medicine, expands the repertoire of potential natural products for renal disease management, and paves new avenues for the development of safe, effective nephroprotectants tailored to oncology settings.

Capitalizing on MHE's established safety profile in non-target organs, this study pioneers the therapeutic application of varying MHE concentrations in a cisplatin-induced AKI model. systematically validate MHE's nephroprotective efficacy against cisplatin toxicity using serum biochemistry and histopathological analysis, and further elucidate its regulatory mechanisms involving oxidative stress and inflammatory pathways. Thus we aimed from this study to investigate and identify a novel natural candidate for mitigating cisplatin nephrotoxicity, and provide robust experimental evidence and a theoretical foundation for the modern pharmacological exploration of traditional Tibetan medicine with a pure academic merit and practical advancing significance for natural product applications in renal disease management.

#### **Material and Methods**

## **Experimental design**

In this study, 50 Kunming mice at 6-8 weeks and with nearly similar body weight were divided by body weight into five layers (10 subjects each), using stratified randomization method to group (random numbers generated through Excel's random function, assigned to five groups with n=10 for each group): a negative control, a murine acute kidney injury model (AKI model control positive group), an MHE lowconcentration treatment (T1=10 mg/kg), an MHE medium-concentration treatment (T2=15 mg/kg), and an MHE high-concentration treatment group (T3=20 mg/kg) (Table 1). The Kunming mice were provided by the Animal Genetic Breeding and Reproduction Laboratory of Xizang Agricultural and Animal Husbandry College and were raised in the college's teaching and practice ranch. The ambient temperature was maintained at 23  $\pm$  5 °C and a 12-hlight/dark cycle, with unrestricted access to distilled water and pathogen-free (SPF) laboratory food. The method of euthanizing the mice adhered to the approved animal protocol (XZA-2025-016) reviewed and authorized by the Animal Welfare and Research Ethics Committee of China Tibet Agricultural and Animal Husbandry University, Xizang, China. The present study followed national guidelines for humane animal treatment and compiled with the relevant legislation.

Table-1. Experimental group design.

| Groups   | Processing method   |    |
|--|---|----|
| Negative control group                                 | Intragastric administration of physiological saline (0.9% NaCl)                     | -  |
| AKI model group (Control Positive)                     | Cisplatin injection (10 mg/kg)+ Intragastric administration of physiological saline | -  |
| MHE low-concentration treatment group (T1=10 mg/kg)    | Cisplatin injection (10 mg/kg) + MHE intragastric administration                    | 10 |
| MHE medium-concentration treatment group (T2=15 mg/kg) | Cisplatin injection (10 mg/kg) + MHE intragastric administration                    | 15 |
| MHE high-concentration treatment group (T3=20 mg/kg)   | Cisplatin injection (10 mg/kg) + MHE intragastric administration                    | 20 |

NOTE: AKI: acute kidney injury; MHE: Mirabilis himalaica extract

# **Reagents and Instruments**

Experimental materials: Roots of *Mirabilis himalaica* (collected from the teaching practice base of Tibet

Agricultural and Animal Husbandry University); Cisplatin (Shandong Keyuan Biochemical Co., Ltd., 99.5%); Hematoxylin-Eosin (HE) staining kit (Beijing Solarbio Science & Technology Co., Ltd., Cat. No.: G1120); Mouse β2-microglobulin (β2-MG) ELISA kit (Jiangsu Meimian Industrial Co., Ltd., Cat. No.: MM-44783M1); Urea/Urea Nitrogen (Urea) Content (Enzyme Method) Detection Kit (Jiangsu Adison Biotechnology Co., Ltd., Item No.: ADS-W-N001-96); Creatinine (CRE) Content (Creatine Oxidase Method) Detection Kit (Jiangsu Adison Biological Technology Co., Ltd., Item Number: ADS-W-FM0034).

Instruments: High speed centrifuge (Gene Company Limited, GZ823516010002), Pipette (Eppendorf, B122161M), Freeze dryer (LaboGene, Model: R507), Microplate reader (TECAN, INFINITE 200 PRO), Embedding machine (Yidi, YD-6LA), Cryostat microtome (Yidi, YD-315III), Biological tissue spreading and baking machine (Yidi, YD-AB3).

## Sample collection and processing

Forty-eight hours after the last dose, whole blood was collected through the method of tail-tip blood sampling, avoiding excessive shaking to prevent hemolysis. Whole blood was left at room temperature for 30 min and centrifuged at 3000×g for 10 min. The supernatant was aspirated using a pipette, avoiding contact with the buffy coat and red blood cells, and transferred to a new centrifuge tube to obtain mouse serum. Serum samples were stored at -20°C to avoid degradation from repeated freeze-thaw cycles.

Using methods compliant with animal ethical standards, experimental mice were euthanized by cervical dislocation and fixed supine on a surgical board. The skin on the chest wall was incised along the midline, and subcutaneous tissue was separated. Sterile surgical instruments were used to isolate the heart, liver, spleen, lungs, and kidneys from surrounding tissues. Intact organs were removed and rinsed with pre-cooled physiological saline to remove residual surface blood. After drying with filter paper, the organs were weighed. The left kidney was fixed in formaldehyde solution for subsequent experiments. This process was performed gently and swiftly to minimize tissue damage while strictly adhering to aseptic procedures to prevent contamination.

#### Preparation of *Mirabilis himalaica* extract

Dried *Mirabilis himalaica* roots were freeze-dried, ground into powder (passed through a 40-mesh sieve; roots were collected simultaneously from the same location and plant part, freeze-dried, and sealed for storage). Powder was mixed with ultra-pure water at a 1:10 (w/v) ratio and decocted twice in a 120 °C water

bath (1 h each time). Supernatants were combined, filtered, and concentrated under reduced pressure to a final concentration of 1 g/mL (raw herb equivalent).

# Establishment of cisplatin-induced acute kidney injury (AKI) model

The optimal modeling concentration was determined by screening six cisplatin concentrations (10, 11, 12, 13, 14, and 15 mg/kg). HE staining revealed significant renal tubular injury at 10 mg/kg (Taghizadeh et al., 2020). Consequently, 10 mg/kg was selected as the modeling concentration (Yamashita et al., 2021). All subsequent AKI model mice received intraperitoneal injections of cisplatin at this dose.

# Gavage method and concentration

Seventy-two hours' post-cisplatin injection, gastric intervention commenced. The negative control and AKI model control positive groups received physiological saline via gavage. Based on similar previous studies, a dose of 10-20 mg/kg of MHE was given to mice (Meng et al., 2020), the MHE treatment groups received: low (10 mg/kg), medium (15 mg/kg), or high-concentration (20 mg/kg) MHE, administered orally once daily for 14 consecutive days.

#### **Detection of renal function indicators**

Serum creatinine (Cr), urea nitrogen (BUN), and  $\beta$ 2-microglobulin ( $\beta$ 2-MG) levels were quantified to systematically evaluate renal excretion, metabolism, and filtration functions.

Creatinine (Cr) was detected spectrophotometrically using the creatine oxidase method (Kit No.: ADS-W-FM043), Urea Nitrogen (BUN) spectrophotometrically by the urease-glutamate dehydrogenase method (Kit No.: ADS-W-N013-96), and  $\beta$ 2-Microglobulin ( $\beta$ 2-MG) by ELISA (Kit No.: MM-44783M1).

# Histopathological analysis of renal tissue

Formaldehyde-fixed left kidneys were paraffinembedded, sectioned (4  $\mu$ m), and stained. Renal tubular epithelial cell swelling, necrosis, and inflammatory cell infiltration were assessed by light microscopy.

Tubular injury was scored in 25 fields from both the upper and lower poles of the kidney on hematoxylin and eosin (H&E)-stained sections (n=10 per group). Each field was assigned a score from 0 to 3 based on

the following histological criteria: 0 for normal histology; 1-3 for the presence of tubular dilation, brush border loss, and accompanying nuclear loss (1 for <1/3 nuclear loss, 2 for 1/3 to 2/3, and 3 for  $\ge 2/3$  nuclear loss) (Yang et al., 2024). To ensure objectivity, all scoring was performed by two independent pathologists who were blinded to the experimental groups.

## **Organ indices**

Thorgan index was calculated for the heart, liver, spleen, lungs, and kidneys:

Organ index (%) = [organ weight (g) / body weight (g)]  $\times$  100

# **Statistical Analysis**

Data are presented as mean ± standard deviation. Statistical analysis was performed using GraphPad Prism 8.0.2 (Abayasekara and Sullo, 2023). Normally

distributed data (Shapiro-Wilk test, P > 0.05) were analyzed by one-way ANOVA with Tukey's post hoc test; non-normally distributed data were analyzed by Kruskal-Wallis test with Dunn's post hoc test.

#### **Results**

# Histopathological repair effect

Pathological changes in kidney tissue were assessed by HE staining (Figures 1 & 2). In the negative control group, kidney tissue exhibited clear architecture, intact glomeruli, tightly arranged renal tubular epithelial cells, and patent lumens (Figures 2A-B). Conversely, the AKI model control positive group displayed collapsed glomerular capillary loops, significant swelling and necrosis of renal tubular epithelial cells, luminal obstruction, and extensive inflammatory cell infiltration (Figures 2C-D). These marked histological differences confirm successful AKI model establishment.

Table-2. Histopathological scoring of tubular injury.

| Groups   | 0 | 1 | 2 | 3 | mean  |
|--|---|---|---|---|-------|
| Negative control group                                 | 7 | 3 | 0 | 0 | 0.3** |
| AKI model group (Control<br>Positive)                  | 0 | 1 | 3 | 6 | 2.5   |
| MHE low-concentration treatment group (T1=10 mg/kg)    | 4 | 3 | 3 | 0 | 0.9** |
| MHE medium-concentration treatment group (T2=15 mg/kg) | 6 | 4 | 0 | 0 | 0.4** |
| MHE high-concentration treatment group (T3=20 mg/kg)   | 0 | 1 | 4 | 5 | 2.4   |

NOTE: 0: none; 1: <1/3 nuclear loss; 2: 1/3 to 2/3; 3:  $\ge 2/3$  nuclear loss. \*\* indicates P < 0.01 compared to the AKI model control positive group, and \* indicates P < 0.05 compared to the AKI model control positive group.

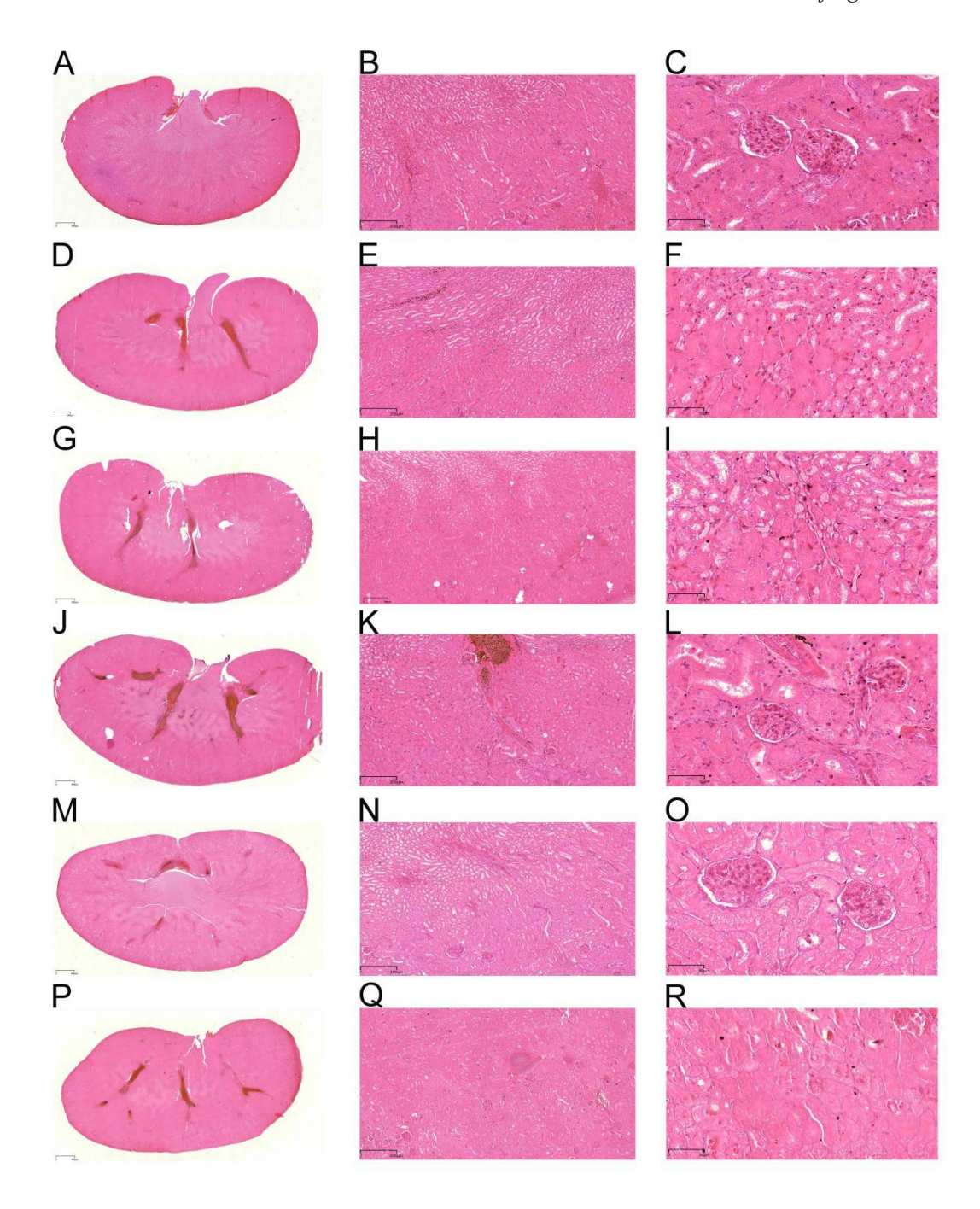


**Figure-1.** Cisplatin concentration gradient-induced HE staining of murine acute kidney injury (from preliminary experiment, n=3). (A-C) 10 mg/kg cisplatin; (D-F) 11 mg/kg cisplatin; (G-I) 12 mg/kg cisplatin; (J-L) 13 mg/kg cisplatin; (M-O) 14 mg/kg cisplatin; (P-R) 15 mg/kg cisplatin.

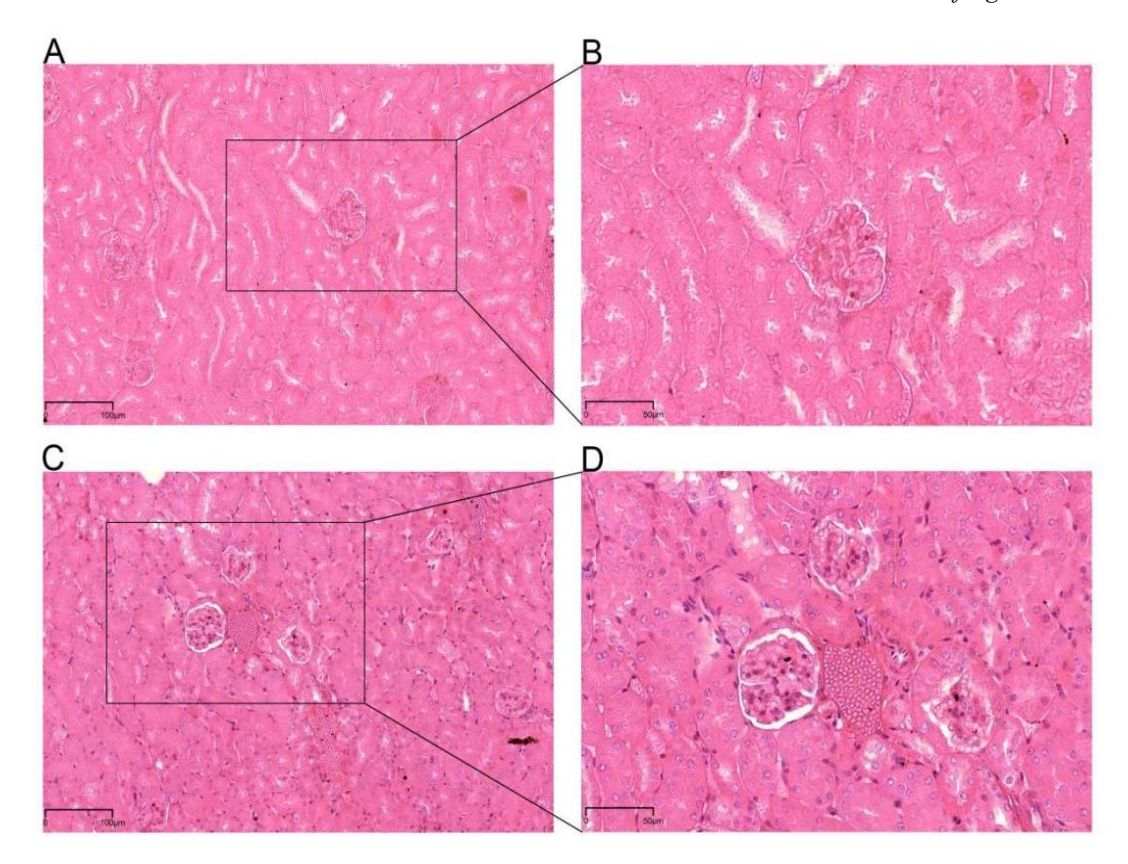


**Figure-2.** Murine acute kidney injury model histology (n=10). (A) Negative control group's mouse kidney (100×); (B) Negative control group's mouse kidney (200×); (C) AKI model control positive group's mouse kidney (100×); (D) AKI model control positive group's mouse kidney (200×).

#### Effects of MHE at different concentrations

Compared to the AKI model control positive group (Figure 3A), MHE intervention significantly ameliorated renal pathology. The MHE low-concentration treatment group (T1=10 mg/kg; Figure 3B) showed reduced renal tubular epithelial cell swelling, sporadic necrotic cells, and diminished

inflammatory infiltration. In the MHE medium-concentration treatment group (T2=15 mg/kg; Fig. 3C), renal tubular architecture was nearly restored, with orderly epithelial cell arrangement, patent lumens, and minimal inflammatory cells. The MHE high-concentration treatment group (T3=20 mg/kg; Figure 3D) exhibited persistent tubular dilation and interstitial fibrosis in some areas.

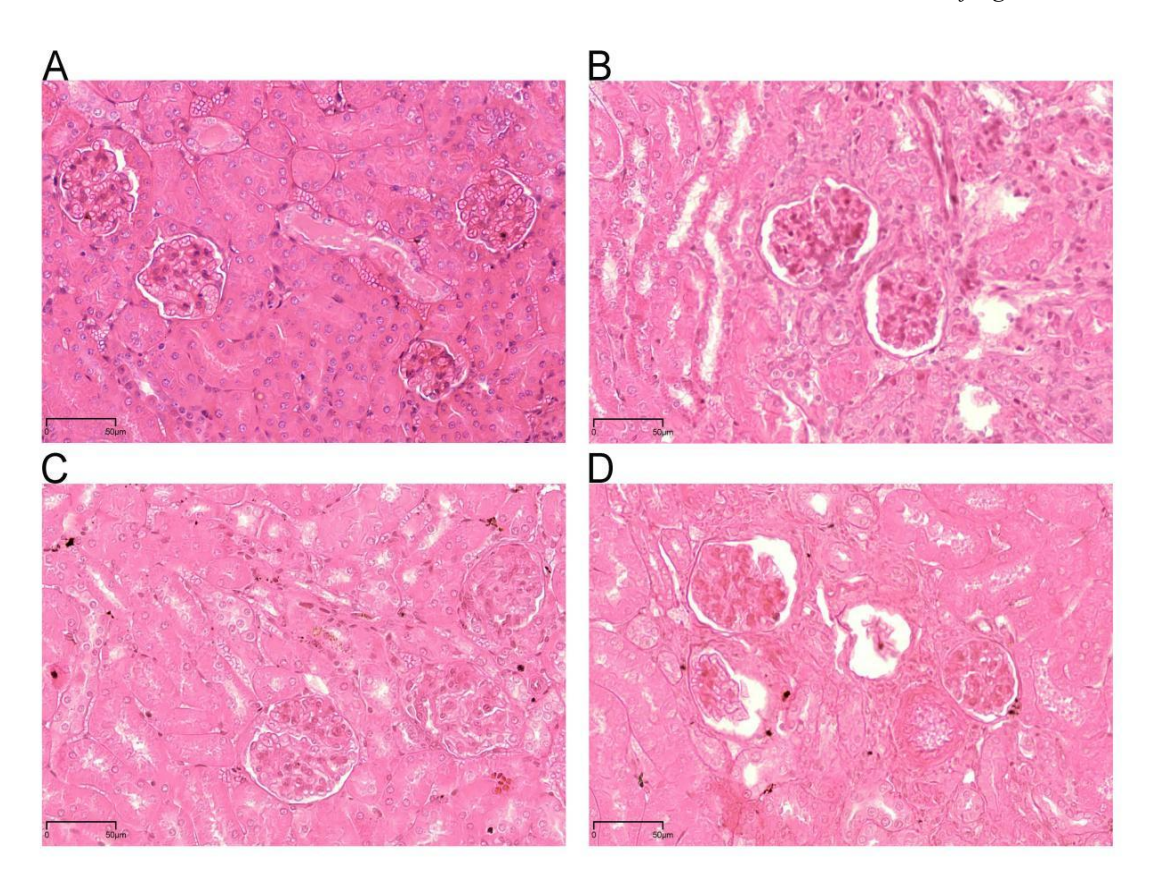


**Figure-3.** Therapeutic effects of *Mirabilis himalaica* extract on murine kidney injury (n=10; 200×). (A) AKI model control positive group; (B) MHE Low-concentration treatment group (T1=10 mg/kg); (C) MHE Medium-concentration treatment group (T2=15 mg/kg); (D) MHE High-concentration treatment group (T3=20 mg/kg).

#### **Renal function biomarkers**

Analysis of serum creatinine (Cr), blood urea nitrogen (BUN), and  $\beta 2$ -microglobulin ( $\beta 2$ -MG) revealed significantly elevated Cr and BUN levels in the AKI model control positive group relative to negative controls, while  $\beta 2$ -MG levels were significantly reduced (Table 2). Following MHE intervention, the MHE low-concentration treatment group (T1=10 mg/kg) exhibited significantly higher  $\beta 2$ -MG levels versus the AKI model control positive group. The MHE medium-concentration treatment group (T2=15 mg/kg) showed significantly lower Cr and BUN levels, and significantly higher  $\beta 2$ -MG levels relative to the AKI model control positive group. The MHE high-concentration treatment group (T3=20 mg/kg)

displayed no significant differences in Cr, BUN, or  $\beta$ 2-MG levels compared to the AKI model control positive group (Table 2).

In our study, the unique nature of the cisplatin-induced renal injury might have led to a complex scenario. Under normal conditions, over 99.9% of  $\beta$ 2-MG, which is freely filtered by the glomeruli, is reabsorbed and metabolized in the renal proximal tubules. However, cisplatin causes extensive damage to proximal tubular cells, resulting in two key impairments: it not only impairs the cells' reabsorption function but also disrupts the intracellular process of  $\beta$ 2-MG degradation. This dual disruption reduces the total amount of  $\beta$ 2-MG undergoing metabolic processing in the initial stage of injury, ultimately leading to a decrease in serum  $\beta$ 2-MG levels.

**Table-3.** Comparison of serum renal function biomarkers between groups (mean  $\pm$  standard deviation).

| Groups                          | Cr (µmol/L)    | BUN (mg/dL)     | <b>β2-MG (μg/L)</b> |
|---------------------------------|----------------|-----------------|---------------------|
| Negative control group          | 12.4±2.27**    | 5.34±0.33*      | 35.52±1.50**        |
| AKI model (Control              | $20.15\pm5.58$ | $6.85 \pm 0.87$ | $28.68\pm2.41$      |
| Positive)group                  |                |                 |                     |
| MHE low-concentration treatment | $14.75\pm2.13$ | $5.76 \pm 0.15$ | 33.57±1.21**        |
| group (T1=10 mg/kg)             |                |                 |                     |
| MHE medium-concentration        | 11.73±0.67**   | 5.17±0.35**     | 34.69±1.33**        |
| treatment group (T2=15 mg/kg)   |                |                 |                     |
| MHE high-concentration          | $17.58\pm1.52$ | $6.05 \pm 0.40$ | $26.36 \pm 1.76$    |
| treatment group (T3=20 mg/kg)   |                |                 |                     |

Note: Data are represented as mean  $\pm$  SEM (n = 10). \*\* indicates P < 0.01 compared to the AKI model control positive group, and \* indicates P < 0.05 compared to the AKI model control positive group.

# Organ index and safety assessment

Organ indices were calculated for five major metabolic/immune organs (Heart, liver, spleen, lungs, kidneys) to evaluate potential MHE toxicity. As

shown in Table 3, no significant intergroup differences in organ indices were observed (P > 0.05), indicating MHE treatment did not induce systemic organ edema or atrophy.

**Table-4.** Comparison of organ indices between groups (mean  $\pm$  standard deviation, %).

| Groups   | heart           | liver           | spleen          | lungs           | kidneys         |
|--|-----------------|-----------------|-----------------|-----------------|-----------------|
| Negative control group                                 | $0.74 \pm 0.15$ | $4.37 \pm 0.45$ | $0.31 \pm 0.14$ | $0.69 \pm 0.09$ | 1.30±0.16*      |
| AKI model (Control Positive )group                     | $0.63 \pm 0.11$ | $4.20 \pm 0.78$ | $0.30\pm0.14$   | $0.77 \pm 0.09$ | $1.06 \pm 0.18$ |
| MHE low-concentration treatment group (T1=10 mg/kg)    | $0.60\pm0.10$   | 4.35±0.24       | $0.27 \pm 0.07$ | $0.75 \pm 0.07$ | $1.08\pm0.10$   |
| MHE medium-concentration treatment group (T2=15 mg/kg) | 0.65±0.12       | 4.19±0.42       | $0.26 \pm 0.06$ | $0.78 \pm 0.05$ | $1.08 \pm 0.08$ |
| MHE high-concentration treatment group (T3=20 mg/kg)   | 0.77±0.24       | 3.86±0.20       | 0.25±0.06       | $0.72\pm0.11$   | 1.05±0.17       |

Note: Data are represented as mean  $\pm$  SEM (n = 10). \*\* indicates P < 0.01 compared to the AKI model control positive group, and \* indicates P < 0.05 compared to the AKI model control positive group.

#### Safety assessment

Through histopathological assessment, the potential toxicity of MHE was systematically evaluated by observing HE-stained sections of critical non-target organs including the heart, liver, and spleen (Figure 4). Results demonstrated that apart from the kidneys, no characteristic morphological alterations indicative of cell necrosis—nor pathological changes such as inflammatory cell infiltration or fibrosis—were observed in the heart (Figures 4A, D, G, J, M), liver

(Figures 4B, E, H, K, N), or spleen (Figures 4C, F, I, L, O) across MHE treatment groups at varying concentrations. Nuclear morphology remained normal, interstitial structures were distinct, tissue layers were well-defined, and cellular arrangement was orderly, aligning with histological features of healthy physiological states. These findings indicate that MHE intervention did not induce systemic organ edema or atrophy in non-target organs under the tested concentrations and experimental duration, confirming its safety for major organs under these conditions.

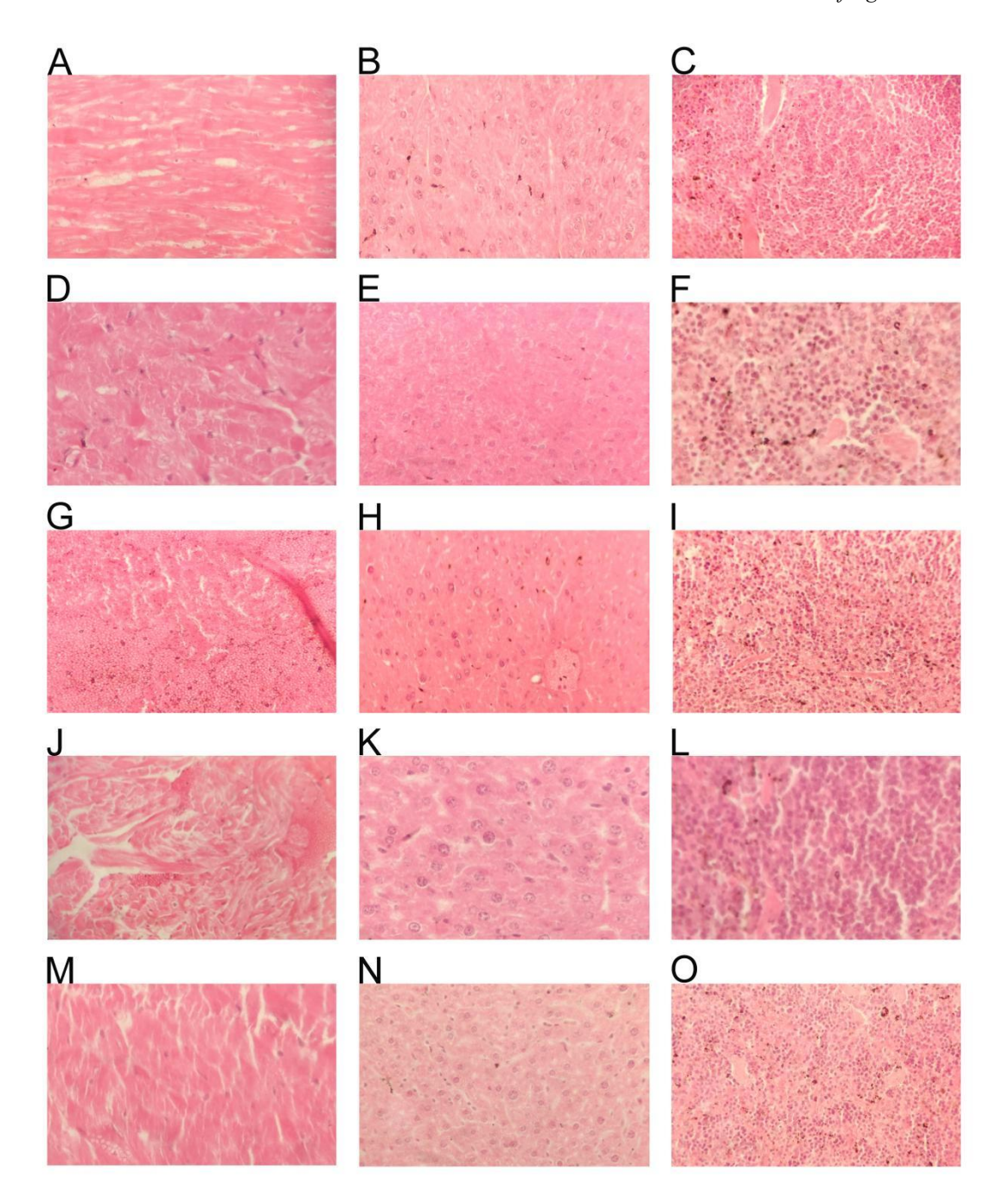


**Figure-4.** Histopathology of non-target organs (n=10). Negative control group: Heart (A), Liver (B), Spleen (C). AKI model control positive group: Heart (D), Liver (E), Spleen (F). MHE low-concentration treatment group (T1=10 mg/kg): Heart (G), Liver (H), Spleen (I). MHE medium-concentration treatment group (T2=15 mg/kg): Heart (J), Liver (K), Spleen (L). MHE high-concentration treatment group (T3=20 mg/kg): Heart (M), Liver (N), Spleen (O).

#### **Discussion**

Cisplatin induces the redox balance of renal tubular epithelial cells by inducing massive generation of reactive oxygen species (ROS), which is one of the core mechanisms leading AKI (Holditch et al., 2019; He et al., 2022). Following renal accumulation, cisplatin impairs mitochondrial respiratory chain function and activates NADPH oxidase, resulting in excessive ROS production (e.g., superoxide anions and hydrogen peroxide). This oxidative stress cascade disrupts intracellular redox homeostasis, ultimately inducing lipid peroxidation, protein carbonylation, and DNA damage.

Our study demonstrated that after intervention with moderate concentration of MHE (15 mg/kg), the creatinine (Cr) and blood urea nitrogen (BUN) levels in the serum of mice in AKI model control positive group were significantly reduced. It was also confirmed through histopathological observation that the aforesaid intervention had significant improving effects on renal damages including degeneration, necrosis and tubular formation of renal tubular epithelial cells (Figure 3). This may be caused by alleviation of the oxidative stress after ROS being eliminated (Zhang et al., 2020). This effect is closely related to flavonoids in MHE (e.g., Boeravinone B/D), which are known to regulate antioxidant signaling pathway (Chen et al., 2021; Zhao et al., 2021; Zhao et al., 2025) Concurrently, such signaling pathway activation contributes to preserving membrane stability (Tognoloni et al., 2023), and maintaining tubular integrity. Supporting this, prior studies have antioxidant-mediated reported histological improvement in cisplatin-AKI models (Chen et al., 2020)(Wang et al., 2021). This result not only confirms the hypothesis that MHE exerts antioxidant protection through Nrf2 pathway, but also provides multi-dimensional theoretical support for explaining the renal protection mechanism of MHE.

Cisplatin also activates NF-κB signaling via IκBα phosphorylation/degradation, subsequently exacerbating tubular inflammation and apoptosis (Zhao et al., 2020; Shareef and Kathem, 2022). Our MHE markedly that showed inflammatory cell infiltration in renal tissues (Figure 3F), achieving histopathology comparable to controls (Figures 2A-B). This anti-inflammatory effect may involve NF-κB or STAT1/4 pathway inhibition, medicine's reflecting traditional multi-target paradigm. Similar mechanism has been reported in the

study on the extract of Astragalus membranaceus in the treatment of diabetic nephropathy: astragalus polysaccharides can reduce renal interstitial inflammation by downregulating the expression levels of TNF-α and IL-6 (Sun et al., 2021). Furthermore, MHE's alkaloids may suppress inflammatory mediator synthesis (Li et al., 2024). Compared with the single pathway inhibitors commonly used in clinical practice (e.g. glucocorticoids), MHE, with its characteristic of synergistic effect of multiple components such as flavonoids and alkaloids, can simultaneously target inflammation for multiple pathological links including inflammatory signaling, oxidative stress apoptosis, demonstrating more comprehensive and precise anti-inflammatory and protective advantages, and providing a new intervention strategy for cisplatin-induced overcoming nephrotoxicity. Cisplatin-induced renal tubular cell apoptosis. mitochondrial mediated primarily through dysfunction, constitutes a pivotal mechanism of acute renal function deterioration. The nephrotoxin disrupts mitochondrial membrane potential, induces cytochrome C release, and activates caspase cascades, culminating in programmed cell death. Central to this process is the dysregulation of Bcl-2 family proteins (e.g., Bax/Bcl-2 ratio imbalance) (Walensky, 2019; Qian et al., 2022; Saddam et al., 2024). Our data demonstrate that medium-concentration MHE (15 mg/kg) markedly attenuated tubular necrosis and improved cellular architecture in AKI models (Figure 3F), suggesting apoptosis inhibition via modulation of apoptotic protein expression. This aligns with established renoprotective mechanisms of natural compounds; for instance, clam peptides exert therapeutic effects by upregulating Bcl-2 while suppressing Bax(Shu et al., 2019). We hypothesize that MHE flavonoids (notably Boeravinone B/D) analogously regulate the Bcl-2/Bax axis to stabilize mitochondrial membranes and inhibit apoptotic signaling, though this requires validation via Western blot or IHC.

Medium-concentration MHE showed significant advantages in improving glomerular filtration function (reduced Cr/BUN), renal tubular reabsorption function (elevated β2-MG), and histopathological parameters (Table 2, Figure 3F). The 15 mg/kg dose likely represents the peak of intestinal absorption and renal distribution efficiency, enabling effective concentrations without metabolic overload(Jiang et al., 2023). Conversely, high-dose MHE (20 mg/kg) paradoxically exacerbated interstitial fibrosis (Figure

3G) and failed to enhance functional markers, mirroring reported flavonoid toxicity at excessive (e.g., Ginkgo biloba-induced vacuolization (Yun-Ying et al., 2019)). This biphasic dose-response underscores the "bell-shaped" efficacy curve characteristic of phytomedicines. Lowconcentration MHE preferentially improved β2-MG (a tubular injury marker), indicating targeted action on tubular reabsorption rather than glomerular filtration. This selectivity may arise from the high membrane permeability of MHE's small-molecule constituents, enabling receptor interaction at low doses. The β2-MG reduction suggests MHE mitigates tubular apoptosis or inflammation, thereby normalizing urinary excretion patterns. By competitively inhibiting cisplatin transporters (e.g., organic cation transporter OCT2), MHE may reduce intracellular cisplatin accumulation (Gong et al., 2020) simultaneously repairing tubular reabsorption barriers through protein expression modulation. This biphasic response parallels observations in Gangban Gui ethanol extract studies for chemical hepatotoxicity (Feng et al., 2017), where low concentrations specifically enhanced hepatocyte membrane stability. Notably, high-concentration MHE (20 mg/kg) failed to improve renal function and induced focal interstitial fibrosis (Figure 3G), indicating metabolic overload at supratherapeutic concentrations (Trevisani et al., 2023).

While this study confirms MHE's renoprotective efficacy against cisplatin-induced AKI and proposes potential mechanisms, four key limitations merit attention for future research. First, mechanistic validation is incomplete: hypotheses (MHE regulating the Bcl-2/Bax axis to inhibit tubular apoptosis; its flavonoids modulating antioxidant pathways) lack direct support (no Western blot/IHC for protein expression, pathway activation, or caspase activity assays). Second, animal models are unrepresentative: a single unspecified murine strain is used, clinical variables (age, comorbidities) are omitted, and only short-term AKI outcomes are evaluated (long-term effects on renal fibrosis/chronic kidney disease unstudied). Third, MHE's active components (flavonoids/alkaloids) and pharmacokinetics are under characterized: no isolation/testing of individual components or critical data (absorption, renal concentration, half-life), hindering explanation of biphasic dose-response and clinical dosing. Fourth, MHE's impact on cisplatin's antitumor efficacy—key for clinical use—is unaddressed. Future work should validate pathways (Western blot/IHC), test MHE in diverse/long-term animal models, characterize its components/pharmacokinetics, and assess effects on cisplatin's antitumor activity to boost translational value.

#### Conclusion

Medium-concentration MHE (15 mg/kg) effectively mitigates cisplatin-induced AKI in mice, significantly reducing serum Cr (11.73±0.67 vs 20.15±5.58 mg/dL, P < 0.01) and BUN (5.17±0.35 vs 6.85±0.87 mg/dL, P < 0.01), improving tubular histopathology, and normalizing  $\beta$ 2-MG excretion (28.68±2.41 vs 34.69±1.33  $\mu$ g/L, P < 0.01), while high-dose MHE showed limited efficacy. The renal-specific effects and organ safety profile confirm its therapeutic potential through multi-target modulation of oxidative stress, inflammation, and apoptosis.

# Acknowledgment

Authors acknowledge the financial support by the Science and Technology Projects of Xizang Autonomous Region, China (XZ202501ZY0147) and Xizang Agriculture and Animal Husbandry University Doctoral Program in Forestry (Phase I) funded by Grant 533325001.

Disclaimer: None.

Conflict of Interest: None.

**Source of Funding:** This research work was funded by the Science and Technology Projects of Xizang Autonomous Region, China (XZ202501ZY0147) and Xizang Agriculture and Animal Husbandry University Doctoral Program in Forestry (Phase I) funded by Grant 533325001.

**Ethical Approval Statement:** All experiments in this study were approved by Animal Welfare and Research Ethics Committee of China Tibet Agriculture and Animal Husbandry University (Approval No. XZA-2025-016).

#### **Contribution of Authors**

Ji J: Writing-original draft preparation.

Ji J & Wang X: Conceptualization, writing, review, and editing, methodology.

Lian S & Nie H: Data curation and writing-editing. Shi F: Software analysis and writing-editing. Peng F & Zhao M: Validation and writing-editing.

Ziauddin: Investigation and writing-editing.

Zhang H & Shang P: Visualization and writingediting, validation, funding acquisition and writingoriginal draft preparation.

Shang P: Resources, supervision, project administration and writing-editing.

All authors read and approved final draft of the manuscript.

#### References

- Abayasekara K and Sullo N, 2023. The clinical use of urinary mitochondrial DNA in adult surgical critical care patients with acute kidney injury. Clin. Exp. Pharmacol. Physiol. 50: 277-286. DOI: https://doi:10.1111/1440-1681.13746.
- Chao Z, Lu H, Xiao F, Shao C, Wei Z, Yu J, Zhang X, Lin L and Tian L, 2020. Robust and tumor-environment-activated DNA cross-linker driving nanoparticle accumulation for enhanced therapeutics. CCS Chemistry 2: 349-361. DOI: https://doi: 10.31635/ccschem.020.202000134.
- Chen L, Cheng H, Kuan Y, Liang T, Chao Y and Lin H, 2021. Therapeutic potential of luteolin on impaired wound healing in streptozotocin-induced rats. Biomedicines 9: 761. DOI: https://doi: 10.3390/biomedicines9070761.
- Chen X, Cao Y, Guo N and Lu G, 2020. Z-ligustilide reduces cisplatin-induced nephrotoxicity via activation of NRF2/HO-1 signaling pathways. Trop. J. Pharm. Res. 19: 1359-1364. DOI: https://doi: 10.4314/tjpr. v19i7.3.
- Chen Z, Shi Y, Zhong F, Zhang K, Zhang F, Xie S, Cheng Z, Zhou Q, Huang Y and Luo H, 2025. Discovery of amentoflavone as a natural PDE4 inhibitor with anti-fibrotic effects. Chin. Chem. Lett. 36: 109956. DOI: https://doi: 10.1016/j.cclet.2024.109956.
- Elmorsy EA, Saber S, Hamad RS, Abdel-Reheim MA, El-Kott AF, AlShehri MA, Morsy K, Salama SA and Youssef ME, 2024. Advances in understanding cisplatin-induced toxicity: molecular mechanisms and protective strategies. Eur. J. Pharm. Sci. 106939. DOI: https://doi: 10.1016/j.ejps.2024.106939.
- Feng Y, Jiao Y and Huang R, 2017. Protective effect of alcohol extract of Yulangsan leaf on chemically-induced liver injury in mice. Trop. J. Pharm. Res. 16: 861-866. DOI: https://doi: 10.4314/tjpr. v16i4.16.

- Gómez-Sierra T, Eugenio-Pérez D, Sánchez-Chinchillas A and Pedraza-Chaverri J, 2018. Role of food-derived antioxidants against cisplatin induced-nephrotoxicity. Food Chem. Toxicol. 120: 230-242. DOI: https://doi: 10.1016/j.fct.2018.07.018.
- Gong T, Liu X, Zhan Z and Wu Q, 2020. Sulforaphane enhances the cisplatin sensitivity through regulating DNA repair and accumulation of intracellular cisplatin in ovarian cancer cells. Exp. Cell Res. 393: 112061. DOI: https://doi: 10.1016/j.yexcr.2020.112061.
- He S, He L, Yan F, Li J, Liao X, Ling M, Jing R and Pan L, 2022. Identification of hub genes associated with acute kidney injury induced by renal ischemia–reperfusion injury in mice. Front. Physiol. 13: 951855. DOI: https://doi: 10.3389/fphys.2022.951855.
- Holditch SJ, Brown CN, Lombardi AM, Nguyen KN and Edelstein CL, 2019. Recent advances in models, mechanisms, biomarkers, and interventions in cisplatin-induced acute kidney injury. Int. J Mol. Sci. 20: 3011. DOI: https://doi: 10.3390/ijms20123011.
- Jiang X, Cai M, Li X, Zhong Q, Li M, Xia Y, Shen Q, Du X and Gan H, 2022. Activation of the Nrf2/ARE signaling pathway protects against palmitic acid-induced renal tubular epithelial cell injury by ameliorating mitochondrial reactive oxygen species-mediated mitochondrial dysfunction. Front. Med. (Lausanne) 9: 939149. DOI: https://doi: 10.3389/fmed.2022.939149.
- Jiang Z, Wu Z, Liu R, Du Q, Fu X, Li M, Kuang Y, Lin S, Wu J and Xie W, 2023. Effect of polymorphisms in drug metabolism and transportation on plasma concentration of atorvastatin and its metabolites in patients with chronic kidney disease. Front. Pharmacol. 14: 1102810. DOI: https://doi: 10.3389/fphar.2023.1102810.
- Li B, Li Z, Liu M, Tian J and Cui Q, 2021. Progress in traditional Chinese medicine against respiratory viruses: A review. Front. Pharmacol. 12: 743623. DOI: https://doi: 10.3389/fphar.2021.743623.
- Li R, Liu H, Liu Y, Guo J, Chen Y, Lan X and Lu C, 2023. Insights into the mechanism underlying UV-B induced flavonoid metabolism in callus of a Tibetan medicinal plant *Mirabilis himalaica*. J. Plant Physiol. 288: 154074. DOI: https://doi: 10.1016/j.jplph.2023.154074.

- Li Z, Liu F, Zeng Y, Liu Y, Luo W, Yuan F, Li S, Li Q, Chen J and Fujita M, 2024. EGCG suppresses PD-1 expression of T cells via inhibiting NF-κB phosphorylation and nuclear translocation. Int. Immunopharmacol. 133: 112069. DOI: https://doi: 10.1016/j.intimp.2024.112069.
- Liu Y, Zhang Z, Li W and Tian S, 2020. PECAM1 combines with CXCR4 to trigger inflammatory cell infiltration and pulpitis progression through activating the NF-κB signaling pathway. Front. Cell Dev. Biol. 8: 593653. DOI: https://doi: 10.3389/fcell.2020.593653.
- Luan X, Zhang L, Li X, Rahman K, Zhang H, Chen H and Zhang W, 2020. Compound-based Chinese medicine formula: From discovery to compatibility mechanism. J. Ethnopharmacol. 254: 112687. DOI: https://doi: 10.1016/j.jep.2020.112687.
- Manohar S and Leung N, 2018. Cisplatin nephrotoxicity: a review of the literature. J. Nephrol. 31: 15-25. DOI: https://doi: 10.1007/s40620-017-0392-z.
- Meng X, Wei M, Wang D, Qu X, Zhang K, Zhang N and Li X, 2020. The protective effect of hesperidin against renal ischemia-reperfusion injury involves the TLR-4/NF-κB/iNOS pathway in rats. Physiol. Int. 107: 82-91. DOI: https://doi: 10.1556/2060.2020.00003.
- Miao N, Wang B, Xu D, Wang Y, Gan X, Zhou L, Xue H, Zhang W, Wang X and Lu L, 2018. Caspase-11 promotes cisplatin-induced renal tubular apoptosis through a caspase-3-dependent pathway. Am. J. Physiol. Renal Physiol. 314: F269-F279. DOI: https://doi: 10.1152/ajprenal.00091.2017.
- Qian S, Wei Z, Yang W, Huang J, Yang Y and Wang J, 2022. The role of BCL-2 family proteins in regulating apoptosis and cancer therapy. Front. Oncol. 12: 985363. DOI: https://doi: 10.1007/s10495-022-01780-7.
- Raghav PK, Kumar R, Kumar V and Raghava GP, 2019. Docking-based approach for identification of mutations that disrupt binding between Bcl-2 and Bax proteins: inducing apoptosis in cancer cells. Mol. Genet. Genomic Med. 7: e910. DOI: https://doi:10.1002/mgg3.910.
- Raudenska M, Balvan J, Fojtu M, Gumulec J and Masarik M, 2019. Unexpected therapeutic effects of cisplatin. Metallomics 11: 1182-1199. DOI: https://doi: 10.1039/c9mt00049f.

- Romani AM, 2022. Cisplatin in cancer treatment. Biochem. Pharmacol. 206: 115323. DOI: https://doi: 10.1016/j.bcp.2022.115323.
- Sablania V, Bosco SJD and Bashir M, 2019. Extraction process optimization of Murraya koenigii leaf extracts and antioxidant properties. J. Food Sci. Technol. 56: 5500-5508. DOI: https://doi: 10.1007/s13197-019-04022-y.
- Saddam M, Paul SK, Habib MA, Fahim MA, Mimi A, Islam S, Paul B and Helal MMU, 2024. Emerging biomarkers and potential therapeutics of the BCL-2 protein family: the apoptotic and antiapoptotic context. Egypt. J. Med. Human Genet. 25: 12. DOI: https://doi: 10.1186/s43042-024-00485-7.
- Shao Y, Peng L, Lin H, Li J, Yu Y, Cao G, Zou H and Yan Y, 2020. Comprehensive investigation of the differences of the roots of wild and cultivated Mirabilis himalaica (Edgew) Heim based on macroscopic and microscopic identification using HPLC fingerprint. Evid. Based Complem. and Altern. Med. 2020: 8626439. DOI: https://doi: 10.1155/2020/8626439.
- Shareef SM and Kathem SH, 2022. Gentiopicroside ameliorates acute inflammatory kidney injury in a mouse model induced by LPS through hampering NF-κB, AP-1 and IRF3 pathways. The FASEB J. 36. DOI: https://doi:10.1096/fasebj.2022.36.s1.17952
- Shu Y, Yang Y, Zhao Y, Ma L, Fu P, Wei T and Zhang L, 2019. Melittin Inducing the Apoptosis of Renal Tubule Epithelial Cells through Upregulation of Bax/Bcl-2 Expression and Activation of TNF-α Signaling Pathway. Biomed. Res. Int. 2019: 9450368. DOI: https://doi: 10.1155/2019/9450368.
- Sugarbaker DJ, Gill RR, Yeap BY, Wolf AS, DaSilva MC, Baldini EH, Bueno R and Richards WG, 2013. Hyperthermic intraoperative pleural cisplatin chemotherapy extends interval to recurrence and survival among low-risk patients with malignant pleural mesothelioma undergoing surgical macroscopic complete resection. J. Thoracic Cardiovasc. Surg. 145: 955-963. DOI: https://doi: 10.1016/j.jtcvs.2012.12.037.
- Sun J, Wei S, Zhang Y and Li J, 2021. Protective effects of astragalus polysaccharide on sepsis-induced acute kidney injury. Anal. Cell Pathol. (Amst) 2021: 7178253. DOI: https://doi: 10.1155/2021/7178253.

- Taghizadeh F, Hosseinimehr SJ, Zargari M, Karimpour Malekshah A and Talebpour Amiri FB, 2020. Gliclazide attenuates cisplatin-induced nephrotoxicity through inhibiting NF-κB and caspase-3 activity. IUBMB Life. 72: 2024-2033. DOI: https://doi: 10.1002/iub.2342.
- Tognoloni A, Bartolini D, Pepe M, Di Meo A, Porcellato I, Guidoni K, Galli F and Chiaradia E, 2023. Platelets rich plasma increases antioxidant defenses of tenocytes via Nrf2 signal pathway. Int. J. Mol. Sci. 24: 13299. DOI: https://doi: 10.3390/ijms241713299.
- Trevisani F, Di Marco F, Quattrini G, Lepori N, Floris M, Valsecchi D, Giordano L, Dell Oca I, Cardellini S and Cinque A, 2023. Acute kidney injury and acute kidney disease in high-dose cisplatin-treated head and neck cancer. Front. Oncol. 13: 1173578. DOI: https://doi: 10.3389/fonc.2023.1173578.
- Walensky LD, 2019. Targeting BAX to drug death directly. Nat. Chem. Biol. 15: 657-665. DOI: https://doi: 10.1038/s41589-019-0306-6.
- Wang Z, Wang L, Luo J and Zhang J, 2021. Protection against acute renal injury by naturally occurring medicines which act through Nrf2 signaling pathway. J. Food Biochem. 45: e13556. DOI: https://doi: 10.1111/jfbc.13556.
- Yamashita N, Nakai K, Nakata T, Nakamura I, Kirita Y, Matoba S, Humphreys BD, Tamagaki K and Kusaba T, 2021. Cumulative DNA damage by repeated low-dose cisplatin injection promotes the transition of acute to chronic kidney injury in mice. Sci. Rep. 11: 20920. DOI: https://doi: 10.1038/s41598-021-00392-6.
- Yang F, Zhu B, Ozols E, Bai H, Jiang M, Ma FY, Nikolic-Paterson DJ and Jiang X, 2024. A gradient model of renal ischemia reperfusion injury to investigate renal interstitial fibrosis. Int. J. Immunopathol. Pharmacol. 38:1210508522 DOI: https://doi:10.1177/03946320241288426.
- Yang J, Li H, Zhang C and Zhou Y, 2022. Indoxyl sulfate reduces Ito, f by activating ROS/MAPK and NF-κB signaling pathways. JCI Insight. 7: e145475. DOI: https://doi: 10.1172/jci.insight.145475.
- Yu S, Gong L, Li N, Pan Y and Zhang L, 2018. Galangin (GG) combined with cisplatin (DDP) to suppress human lung cancer by inhibition of

- STAT3-regulated NF-κB and Bcl-2/Bax signaling pathways. Biomed. Pharmacother. 97: 213-224. DOI: https://doi: 10.1016/j.biopha.2017.10.059.
- Yun-Ying LI, Xiao-Yan LU, Jia-Li S, Qing-Qing W, Zhang Y, Zhang J and Xiao-Hui F, 2019. Potential hepatic and renal toxicity induced by the biflavonoids from Ginkgo biloba. Chin J. Nat. Med. 17: 672-681. DOI: https://doi: 10.1016/S1875-5364(19)30081-0.
- Zhang Y, Chen Y, Li B, Ding P, Jin D, Hou S, Cai X and Sheng X, 2020. The effect of monotropein on alleviating cisplatin-induced acute kidney injury by inhibiting oxidative damage, inflammation and apoptosis. Biomed. Pharmacother. 129: 110408. DOI: https://doi: 10.1016/j.biopha.2020.110408.
- Zhao H, Zhang R, Yan X and Fan K, 2021. Superoxide dismutase nanozymes: an emerging star for antioxidation. J. Mater. Chem. B. 9: 6939-6957. DOI: https://doi: 10.1039/d1tb00720c.
- Zhao Q, Yang F, Meng L, Chen D, Wang M, Lu X, Chen D, Jiang Y and Xing N, 2020. Lycopene attenuates chronic prostatitis/chronic pelvic pain syndrome by inhibiting oxidative stress and inflammation via the interaction of NF-κB, MAPKs, and Nrf2 signaling pathways in rats. Andrology 8: 747-755. DOI: https://doi: 10.1111/andr.12747.
- Zhao Y, Tian X, Yan Y, Tian S, Liu D and Xu J, 2025. Lithospermic acid alleviates oxidative stress and inflammation in DSS-induced colitis through Nrf2. Eur. J. Pharmacol. 177390. DOI: https://doi: 10.1016/j.ejphar.2025.177390.
- Zhao Z, Wu Q, Xu Y, Qin Y, Pan R, Meng Q and Li S, 2024. Groenlandicine enhances cisplatin sensitivity in cisplatin-resistant osteosarcoma cells through the BAX/Bcl-2/Caspase-9/Caspase-3 pathway. J. Bone Oncol. 48: 100631. DOI: https://doi: 10.1016/j.jbo.2024.100631.
- Zhu X, Li J, Tang Y, Li X, Xu J, Jing R and Liu T, 2023. Acute kidney injury after multiple cycles of cisplatin chemotherapy: A nomogram for risk assessment. Kidney Blood Press. Res. 48: 485-494. DOI: https://doi: 10.1159/000531289.